



LUND UNIVERSITY

On Using Wind Speed Preview to Reduce Wind Turbine Tower Oscillations

Kristalny, Maxim; Madjidian, Daria; Knudsen, Torben

Published in:
IEEE Transactions on Control Systems Technology

DOI:
[10.1109/TCST.2013.2261070](https://doi.org/10.1109/TCST.2013.2261070)

2013

[Link to publication](#)

Citation for published version (APA):
Kristalny, M., Madjidian, D., & Knudsen, T. (2013). On Using Wind Speed Preview to Reduce Wind Turbine Tower Oscillations. *IEEE Transactions on Control Systems Technology*, 21(4), 1191-1198.
<https://doi.org/10.1109/TCST.2013.2261070>

Total number of authors:
3

General rights

Unless other specific re-use rights are stated the following general rights apply:
Copyright and moral rights for the publications made accessible in the public portal are retained by the authors and/or other copyright owners and it is a condition of accessing publications that users recognise and abide by the legal requirements associated with these rights.

- Users may download and print one copy of any publication from the public portal for the purpose of private study or research.
- You may not further distribute the material or use it for any profit-making activity or commercial gain
- You may freely distribute the URL identifying the publication in the public portal

Read more about Creative commons licenses: <https://creativecommons.org/licenses/>

Take down policy

If you believe that this document breaches copyright please contact us providing details, and we will remove access to the work immediately and investigate your claim.

LUND UNIVERSITY

PO Box 117
221 00 Lund
+46 46-222 00 00

On Using Wind Speed Preview to Reduce Wind Turbine Tower Oscillations

Maxim Kristalny[†], Daria Madjidian[†] and Torben Knudsen[‡]

Abstract—We investigate the potential of using previewed wind speed measurements for damping wind turbine fore-aft tower oscillations. Using recent results on continuous-time H^2 preview control, we develop a numerically efficient framework for the feedforward controller synthesis. One of the major benefits of the proposed framework is that it allows us to account for measurement distortion. This results in a controller that is tailored to the quality of the previewed data. A simple yet meaningful parametric model of the measurement distortion is proposed and used to analyze the effects of distortion characteristics on the achievable performance and on the required length of preview. We demonstrate the importance of accounting for the distortion in the controller synthesis and quantify the potential benefits of using previewed information by means of simulations based on real-world turbine data.

I. INTRODUCTION

An evident trend in the area of wind energy during the past decades is a continuous growth of wind turbine dimensions. Modern day commercial turbines typically stand more than 90 m tall, with a blade span of over 120 m [1]. As a consequence of such a large size, structural loads experienced by turbines becomes a central issue. These loads shorten the life span of the turbine and increase its maintenance costs. Alternatively, turbines with a higher tolerance to structural loads require a more rigid structure and, as a result, higher construction costs. For this reason, load reduction is an important factor in decreasing the cost of wind energy.

In this paper, we focus on exploiting wind speed preview for reducing tower fore-aft oscillations in wind turbines with collective pitch control. The idea of using preview in the control of wind turbines was discussed in [1], [2] and has been a subject of interest for many researchers in the last few years. The use of preview in cyclic pitch control was considered in [3]. Model predictive control with preview was studied in a collective pitch setting in [4], [5] and in an individual pitch setting in [6]. The benefit of model predictive techniques is in their ability to account for hard input, output and state constraints, which is particularly useful when operating near rated conditions. These methods, however, may require heavy online computations and impede the analysis of the problem. The use of preview in individual pitch control was considered in [7] using the LMI approach to H^∞ optimization. In [8], [9], preview control for load reduction was studied using model inversion methods and adaptive control algorithms based on recursive least squares.

To the best of our knowledge, the methods proposed so far rely on time discretization. Availability of preview is typically handled by a state augmentation procedure, which leads to a finite-dimensional, yet, high-order optimization. In spite of its conceptual simplicity, this approach may have a number of drawbacks. In particular, it impedes direct analysis of the problem and is associated with a high computational burden, which grows with the increase of the preview length.

A different approach is proposed in this paper. We show that the problem can be conveniently formulated as an instance of the continuous-time two-sided H^2 model matching optimization with preview, which was recently solved in [10]. Unlike the commonly used discrete-time methods, the computational burden of the proposed solution does not depend on the preview length. The resulting optimal controller has an interpretable structure and is easy to implement. Moreover, the proposed method facilitates the analysis of the problem, which is the main topic of this work.

A large part of the paper is devoted to the analysis of the effects of measurement distortion on the feedforward control. An important feature of the proposed method is that it allows us to include the distortion model in the problem formulation and to account for it in the controller synthesis procedure. This results in a feedforward controller that is tailored to the quality of the previewed information, and facilitates the analysis of the influence of distortion on the feedforward control. A simple and intuitive parametric model for the distortion is proposed and used to study the effects of distortion characteristics on the achievable performance and on the required length of preview. Using simulations based on real wind turbine measurements, we demonstrate that accounting for measurement distortion in the controller design is crucial in order to properly take advantage of the previewed wind speed information.

In the last part of the paper, we consider the possibility of obtaining a preview of the wind speed from upwind turbines in a wind farm. This idea was previously proposed in [11] as a possible alternative to the LIDAR based control. By analyzing data collected from a wind farm, we show that, at least in the setup proposed in [11], this idea is not likely to work. The results indicate that due to the large distance between neighboring turbines, the wind speed fluctuations experienced by two turbines are correlated only at lower frequencies, which are not pertinent to load reduction.

The paper is organized as follows: Section II describes the turbine model and the model of the wind speed. The problem formulation and solution are presented in Section III. Section IV constitutes the main part of this paper.

[†]Department of Automatic Control, Lund University, Box 118, SE-221 00 Lund, Sweden. E-mail: {maxim,daria}@control.lth.se

[‡]Automation and Control, Department of Electronic Systems, Aalborg University, Fredrik Bajers Vej 7, DK-9220 Aalborg Ø, Denmark. E-mail: tk@es.aau.dk

It is devoted to analyzing the benefits of using previewed wind speed measurements and the effects of measurement distortion. In Section V, we look into using previewed wind speed measurements from upwind turbines. Finally, some concluding remarks are provided in Section VI.

Notation: The Frobenius norm of a matrix, A , is denoted by $\|A\|_F$. The space of all proper and stable transfer matrices is denoted by H^∞ . The space of all rational transfer matrices in H^∞ is denoted by RH^∞ . Given a transfer matrix $G(s)$, its conjugate is denoted by $G^\sim(s) := [G(-s)]'$. For any rational strictly proper transfer function given by its state-space realization

$$G(s) = C(sI - A)^{-1}B = \left[\begin{array}{c|c} A & B \\ \hline C & 0 \end{array} \right],$$

the completion operator, [12], is defined as

$$\pi_h\{G(s)\} := Ce^{-Ah}(sI - A)^{-1}B - e^{-sh}C(sI - A)^{-1}B$$

and is an FIR (finite impulse response) linear system.

II. MODELING

A. Turbine model

We adopt a nonlinear aeroelastic model of a 5 MW NREL wind turbine from [13]. The model consists of a tower with two fore-aft and two side-to-side bending modes, three blades with two flapwise and one edgewise bending modes each, a 3rd order drive train, as well as the internal controller described in [13] and modified according to [14]. In addition, the model has been augmented with a 1st order generator model and a 2nd order pitch actuator with an internal delay, which were both adopted from [14].

The internal controller manipulates the generator torque and blade pitch angle in order to meet a prescribed power demand. It has three main modes of operation, usually called “operating regions”. The first two modes are identical to those described in [13], whereas the third mode is extended according to [14] in order to provide the capability for derated operation. The controller operates in the third (derated) mode if the power demand does not exceed the power that can be captured by the turbine. In this mode, excess wind power is curtailed in order to satisfy demand. This is achieved by keeping the rotor speed close to its rated value by adjusting the pitch angle, and manipulating the generator torque in order to maintain the desired power. Throughout this paper, we will assume that the power demand does not exceed the power available in the wind, which means that the internal controller operates in derated mode.

We use the full nonlinear turbine model described above for simulation purposes only. For analysis and controller synthesis, a simplified linearized version of this model is adopted from [15]. The nominal mean wind speed and power demand are denoted by V_{nom} and p_{nom} , respectively. Throughout this paper, we assume that $V_{\text{nom}} = 10$ m/sec and

$p_{\text{nom}} = 2$ MW. A continuous-time linearized wind turbine model can be described by the block depicted in Figure 1. It can be partitioned as $P = \begin{bmatrix} P_V & P_u \end{bmatrix}$ with respect to the two input signals. The inputs V and p_{ref} denote deviations in the wind speed and the power demand from their nominal values. The second input will also be denoted as $u := p_{\text{ref}}$. Note that in the considered setting, u is the only available control signal. The linearized model neglects generator dynamics, which makes the actual deviation in power production equal to p_{ref} . The three outputs of P are denoted by F , ω , and β and stand for the deviations in the thrust force, rotor speed, and pitch angle, respectively. The vector containing all outputs of the system is denoted by $z := \begin{bmatrix} F & \omega & \beta \end{bmatrix}'$. The state-space realization of P for the aforementioned operating point is given by

$$P = \left[\begin{array}{ccc|cc} 0 & 1.2 \cdot 10^2 & -9.2 \cdot 10^{-1} & 0 & 0 \\ -8.4 \cdot 10^{-3} & -3.2 \cdot 10^{-2} & 0 & 1.6 \cdot 10^{-2} & -2.1 \cdot 10^{-8} \\ 0 & 1.5 \cdot 10^2 & -1.6 & 0 & 0 \\ \hline -5.8 \cdot 10^4 & -1.5 \cdot 10^5 & 0 & 7.4 \cdot 10^4 & 0 \\ 0 & 1 & 0 & 0 & 0 \\ 1 & 0 & 0 & 0 & 0 \end{array} \right],$$

where the three states correspond to the pitch angle, rotor speed and an internal controller state.

This linearized model neglects the influence of tower oscillations on the wind speed experienced by the turbine. Instead, we consider tower oscillations as an external dynamical mode excited by the thrust force. It is approximated by a second order system with static gain $k_{\text{twr}} = 3.58 \times 10^{-7}$, natural frequency $\omega_{\text{twr}} = 2$ rad/sec and damping coefficient $\zeta_{\text{twr}} = 0.08$, which is consistent with [13]. The tower deflection, i.e., the displacement of the nacelle, will hereafter be denoted by y .

Remark 1: Note that considering a turbine equipped with a standard internal controller is restrictive. This rules out direct access to the pitch and the generator torque, restricts us to work in a derated mode and leaves the power reference as the only available control signal. At the same time, this simplifies the problem and facilitates experiments on existing wind turbines. It is worth emphasizing that the ideas, the problem formulation and the solution techniques discussed in the paper can be extended to more general situations with no internal controller, individual pitch capabilities and a wide range of structural loads being in focus.

B. Wind model

Since the relevant system variables such as rotor speed, thrust force and nacelle displacement depend on the wind speed variations along the entire rotor, we adopt the concept of *effective wind speed* (EWS) from [16]. It can be interpreted as a spatially constant wind field that produces a similar rotor torque and thrust force as the actual spatially varying wind flow. To model EWS at a turbine we use real wind turbine data collected from the Egmond aan Zee Offshore Wind Farm (OWEZ) [17]. During the period of data collection, the mean wind speed was 10 m/s, which

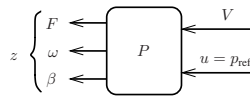


Fig. 1. Turbine model

is consistent with the operating point in Section II-A. For more information on the data set we refer to [16] where it is described in detail.

To estimate EWS, we used the time varying extended Kalman filter described in [16]. A 10 minute sample of the estimated EWS deviation from its nominal value is shown in Figure 2, where it can be compared to the deviation of the measured nacelle wind speed. As expected, the EWS fluctuates less than the point wind speed measured on the nacelle.

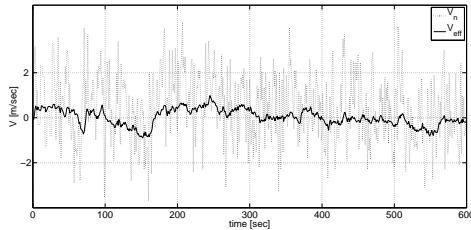


Fig. 2. Comparison between measured nacelle wind speed, V_n , and estimated effective wind speed, V_{eff} . As expected, V_{eff} fluctuates less than V_n .

Based on the estimated EWS a model was identified using a prediction error method [18]. The model is given by a signal generator M_V , which takes white noise with unit intensity as input and provides the wind speed signal as the output. A first order model proved to be sufficient and is presented below:

$$M_V = \frac{7.4476}{(1/0.0143)s + 1}.$$

III. PROBLEM FORMULATION AND SOLUTION

The problem of using wind speed measurements for load reduction naturally falls into the open-loop disturbance attenuation scheme, depicted in Figure 3. The effective

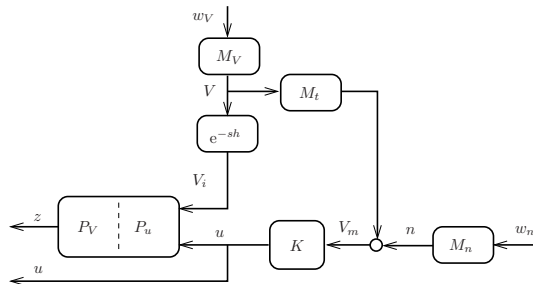


Fig. 3. Turbine control scheme

wind speed deviation V acts as an external disturbance. Its frequency content is modeled by the filter M_V as described in Section II-B. The controller K receives a measurement of the wind speed denoted by V_m . The delay h in the first input of the plant corresponds to the length of preview available to the controller. Since the wind speed is measured some distance ahead of the turbine, there will always be a mismatch between V_m and the actual wind experienced by the turbine V_i . To account for this, we introduce the

additive noise n , which, together with the filters M_t and M_n , model distortion between the experienced and the measured wind speeds. A detailed discussion on the choice of M_t and M_n will be provided in Section IV-B. The aim of the controller is to keep the components of z small. Pitch activity should be kept low to reduce wear on the pitch mechanism. Deviations of rotor speed from its rated value should not be large due to mechanical design constraints. Finally, fluctuations in thrust force should be alleviated, since they introduce oscillations, which cause damage to the tower, blades and other mechanical components [19]. To prevent large fluctuations in produced power, the control signal u should also be penalized.

The relation between the input and output signals in Figure 3 is given by:

$$\begin{bmatrix} z/w_V & z/w_n \\ u/w_V & u/w_n \end{bmatrix} = \begin{bmatrix} e^{-sh} P_V M_V & 0 \\ 0 & 0 \end{bmatrix} + \begin{bmatrix} P_u \\ 1 \end{bmatrix} K \begin{bmatrix} M_t M_V \\ M_n \end{bmatrix}'.$$

We define the cost transfer function for the optimization as

$$T := \begin{bmatrix} W_z & 0 \\ 0 & W_u \end{bmatrix} \begin{bmatrix} z/w_V & z/w_n \\ u/w_V & u/w_n \end{bmatrix},$$

where $W_z = \text{diag}\{W_F, W_w, W_\beta\}$ contains weights for all the components of z , and W_u is the weight for the power reference. We choose the weight of the thrust force as

$$W_F = k_F \frac{s + \omega_{\text{twr}}}{s^2 + 2\zeta_{\text{twr}}\omega_{\text{twr}}s + \omega_{\text{twr}}^2}$$

in order to penalize tower oscillations. The weight for the rotor speed is static $W_w = k_w$. In order to penalize high pitch rates, we choose the weight for the pitch angle as a high-pass filter

$$W_\beta = k_\beta \frac{s}{s + \omega_\beta}.$$

Finally, we choose the weight for the power reference as

$$W_u = k_u \frac{(s + \omega_{\text{twr}})^2}{s^2 + 2\zeta_{\text{twr}}\omega_{\text{twr}}s + \omega_{\text{twr}}^2}$$

in order to prevent the controller from damping tower oscillations by means of oscillations in power production and, as a result, in the pitch angle.

Defining the transfer matrices

$$\left[\begin{array}{c|c} G_1 & G_3 \\ \hline G_2 & 0 \end{array} \right] := \left[\begin{array}{c|c|c} W_z P_V M_V & 0 & W_z P_u \\ \hline 0 & 0 & W_u \\ \hline M_t M_V & M_n & 0 \end{array} \right] \quad (1)$$

and choosing $\|T\|_2$ as the performance criterion, the problem can be formulated as model matching optimization.

OP: Given $G_1, G_2, G_3 \in RH^\infty$ as defined in (1) and the preview length $h > 0$ find $K \in H^\infty$, which guarantees

$$T = e^{-sh}G_1 - G_3KG_2 \in H^2 \quad (2)$$

and minimizes $\|T\|_2$.

The formulation above can be considered as a special case of a more general problem, whose solution was recently obtained in [10]. Below, we tailor this solution to **OP**.

Consider the composite *finite-dimensional* system given by its minimal state-space realization

$$\begin{bmatrix} G_1 & G_3 \\ G_2 & 0 \end{bmatrix} = \left[\begin{array}{c|cc} A & B_1 & B_2 \\ \hline C_1 & 0 & D_3 \\ C_2 & D_2 & 0 \end{array} \right].$$

Assume that

\mathcal{A}_1 : $D_2 D_2' = I$ and $D_3' D_3 = I$,

\mathcal{A}_2 : $G_2(s)$ and $G_3(s)$ have no $j\omega$ -axis transmission zeros.

These are the standard assumptions in H^2 optimal control that rule out redundancy and singularity of the problem. The following result provides a complete state-space solution of **OP** in terms of two algebraic Riccati equations (AREs).

Theorem 1: If the assumptions \mathcal{A}_{1-2} hold, then **OP** has a unique solution given by

$$K^{\text{opt}} = -e^{-sh} \left[\frac{\bar{A}}{F} \middle| \frac{L}{0} \right] - \left[\frac{\bar{A}}{F} \middle| \frac{B_2}{I} \right] \pi_h \{ \tilde{G} \} \left[\frac{\bar{A}}{C_2} \middle| \frac{L}{I} \right],$$

where $\bar{A} := A + B_2 F + L C_2$ and

$$\tilde{G} := \left[\begin{array}{cc|c} -(A + B_2 F)' & (C_1 + D_3 F)' C_1 Y & X L \\ 0 & -(A + L C_2)' & C_2' \\ \hline B_2' & -D_3' C_1 Y & 0 \end{array} \right]$$

with $F := -B_2' X - D_3' C_1$ and $L := -Y C_2' - B_1 D_2'$, ere $X \geq 0$ and $Y \geq 0$ are the stabilizing solutions of the algebraic Riccati equations

$$\begin{aligned} A'X + XA - (XB_2 + C_1' D_3)(B_2'X + D_3' C_1) + C_1' C_1 &= 0 \\ AY + YA' - (YC_2' + B_1 D_2')(C_2 Y + D_2 B_1') + B_1 B_1' &= 0. \end{aligned}$$

Moreover, the expression for the performance achieved by the optimal controller is given by

$$\|T^{\text{opt}}\|_2^2 = \left\| \left[\begin{array}{cc|c} A & B_2 F & B_1 \\ \hline -L C_2 & \bar{A} & -L D_2 \\ C_1 & D_3 F & 0 \end{array} \right] \right\|_2^2 - \|\pi_h \{ \tilde{G} \}\|_2^2,$$

Proof: This is a special case of [10, Theorem 2] with stable G_1 , G_2 and G_3 . ■

It is worth stressing that the computational load of the solution provided in Theorem 1 does not depend on the preview length. In fact, it is based on the standard AREs associated with the preview-free problem.

Also note that the solution provides an insight into the structure of the optimal controller. It is easy to see that the first term of K^{opt} is based on the optimal controller for the preview-free problem. In fact, as manifested by the presence of the delay element, this term “ignores” the existence of previewed information. Availability of preview is accounted for solely by the second term, in which the only component that depends on the preview length is the FIR block $\pi_h \{ \tilde{G} \}$.

Finally, the result in Theorem 1 facilitates the analysis of the influence of preview length on the achievable performance. Let $\mathcal{P}_h = \|T^{\text{opt}}\|_2$ be the optimal performances achieved with h seconds of preview. It can be verified that $\mathcal{P}_h^2 := \mathcal{P}_0^2 - \|\pi_h \{ \tilde{G} \}\|_2^2$. The first term in the above expression stands for the optimal performance with $h = 0$, while the second term corresponds to the performance improvement due to availability of preview. The latter can be computed using the integral $\|\pi_h \{ \tilde{G} \}\|_2^2 = \int_0^h \|\tilde{G}^{\sim}(t)\|_F^2 dt$,

where $\tilde{G}^{\sim}(t)$ refers to the impulse response of the stable finite-dimensional system $(\tilde{G})^{\sim}$. This shows that one can construct the curve of \mathcal{P}_h versus h without solving the problem for each value of preview length but only at the expense of solving two AREs.

Remark 2: Note that the proposed framework allows us to synthesize a preview controller for a specific operating point. In practice, the controller will need to be continuously adapted to the changes in operating point and, perhaps, also in the stochastic characteristics of the wind. The method of adding such adaptation capabilities to the controller deserves a separate discussion and is a possible direction for future work.

IV. ANALYSIS AND SIMULATIONS

In this section, we use the mathematical framework described in Section III in order to assess the potential of exploiting previewed measurements of the effective wind speed for reducing tower oscillations. In particular, we examine the influence of the preview length and measurement distortion on the achievable performance.

All simulations in this section are performed on the complete nonlinear model¹ described in the beginning of Section II-A. We choose the weight parameters used in the definition of the performance criteria in Section III as

$$\begin{aligned} k_V &= 1, \quad k_n = 1 \times 10^{-3}, \quad k_u = 1.8 \times 10^{-2}, \\ k_F &= 0.5, \quad k_w = 2 \times 10^6. \end{aligned}$$

This section is divided into three parts. In Section IV-A, we assume that perfect measurements of the wind speed are available to the controller. This enables us to find an upper bound of the achievable performance. In Section IV-B, we introduce measurement distortion and observe its effect on the behavior of different controllers. In particular, we show the importance of taking distortion into account during the controller design. Finally, in Section IV-C, we analyze the influence of the distortion on the achievable performance and the required length of preview.

A. Preview control with perfect measurements

As a first step, let the distortion model be $M_t = 1$ and $M_n = 3 \times 10^{-3}$. This corresponds to the situation in which the controller receives (almost) perfect measurements of the incoming wind speed with a preview of h seconds.

The natural questions when using preview are whether it can yield a noticeable performance improvement, and if so, what length of preview it requires. To address these questions, a curve of the achievable performance as a function of the preview length is presented in Figure 4. The values are normalized with respect to the performance of the original system without feedforward control. The figure indicates that in the considered setup with perfect measurements the reasonable scale of preview length is a number of seconds.

¹The model is implemented using NREL's FAST simulation package [20] and Simulink®. The FAST input files used in the simulation are described in detail in [13] and the parameter settings for the internal controller, pitch actuator, and generator can be found in [21].

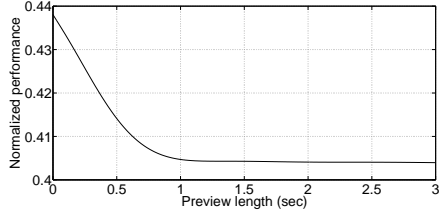


Fig. 4. Achievable performance vs. preview length for the case of perfect measurement (normalized with respect to original system performance). We see that the reasonable scale of preview length is a number of seconds. In fact, 90% of all possible improvement is achieved with $h = 0.75$ sec.

In fact, 90% of all possible improvement is achieved with a preview of 0.75 sec.

Below we will compare the behaviour of the following three systems:

- 1) The original system without feedforward control, namely, with $K = 0$.
- 2) The system with feedforward controller based on local measurements without preview. This controller will be denoted by K_0^p and is obtained by solving **OP** for $h = 0$.
- 3) The system with feedforward controller based on measurements with preview of $h = 1.3$ sec². This controller will be denoted by K_h^p .

Remark 3: The superscript p in K_0^p , K_h^p reflects that these controllers were synthesized assuming availability of perfect measurements.

We simulate the response of these three systems to the effective wind speed estimated from real-world data as explained in Section II-B. We run simulations on 10 different time series, each one minute long. The time series from one of the simulations are shown in Figure 5. The average outcome is presented in Table I, where the DEL notation represents the 1 Hz *damage equivalent load*. This is a constant amplitude sinusoidal load that causes the same fatigue damage during one minute as the original load history does, see [15], [22], [19] for more details. The DELs listed in Table I are for the fore-aft tower base bending moment, denoted M_t , and the flapwise blade root bending moment, denoted M_b . The tower base DEL was computed using an S/N-slope of 4 which is representative of steel structures, and the blade root DEL was computed with an S/N-slope of 10 which is representative of materials made out of glass fiber [23]. $\text{DEL}(M_b)$ was included due to the coupling between tower and blade bending modes [19].

As expected, feedforward both with and without preview significantly reduces the tower bending moment. Both of these controllers also succeed in reducing the blade bending moment, the pitch rate, as well as the magnitude of the rotor speed deviations.

Inspecting the last two rows in Table I, we see that the benefit of using previewed information is substantial.

²A relatively long preview ($h > 0.75$ sec) is chosen in order to facilitate comparison of the resulting controller with those designed in the following subsection.

TABLE I
SIMULATION RESULTS BASED ON THE NONLINEAR TURBINE MODEL AND EWS ESTIMATED FROM REAL-WORLD DATA. (FEEDFORWARD BASED ON PERFECT EWS MEASUREMENTS.)

	DEL(M_t) kNm	DEL(M_b) kNm	max($\dot{\beta}$) deg/sec	max(P) kW	max(ω) rpm
$K = 0$	3581	996	0.33	0	5.5×10^{-2}
K_0^p	1861	777	0.15	267	2.4×10^{-2}
K_h^p	1280	734	0.17	222	2.7×10^{-2}

Comparing the tower bending moment for the two feedforward controllers, we see that preview offers improvement of approximately 31%.

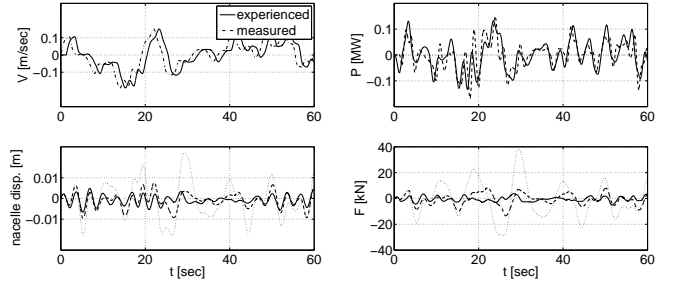


Fig. 5. Simulation results based on the nonlinear turbine model and EWS estimated from real-world data. The results illustrate the behavior of controllers designed assuming perfect wind measurements. [dotted — $K = 0$; dashed — K_0^p ; solid — K_h^p] The average results of 10 simulations of this kind are summarized in Table I.

B. Preview control with distorted measurements

The results so far were based on perfect measurements of the incoming wind speed. This assumption is not realistic, especially taking into account that to obtain preview, one needs to measure the wind speed some distance ahead of the turbine. As the wind travels from the measuring location to the turbine, its high frequency content will be distorted, [24]. As a result, one would expect that the longer the preview in our measurements, the more distortion they may experience. This question was investigated in [25] in the context of LIDAR based wind speed measurements.

For the purposes of this work, we propose a simple, yet intuitive parameterized model for the distortion. To account for distant sensing, we may choose M_t and M_n as

$$M_t(s) = \frac{\omega_t}{s + \omega_t}, \quad (3)$$

$$M_n(s) = \frac{s}{s + \omega_t} M_V. \quad (4)$$

In this setup, the high-frequency component of V is filtered out by M_t and then replaced using the uncorrelated signal generator n , see Figure 3. The idea behind the parameterization (3)-(4) is to obtain equal spectral properties for the effective wind speeds at the measurement and the turbine locations. Indeed, with this choice of M_t and M_n the spectral densities of V_i and V_m will be equal, since

$$|M_t(j\omega)|^2 |M_V(j\omega)|^2 + |M_n(j\omega)|^2 = |M_V(j\omega)|^2.$$

Note, however, that in addition to the distortion due to the distant sensing, the signal V_m will inevitably be corrupted by some sensor noise. For simplicity, we assume that the sensor noise is white and account for it by adding a constant component to M_n , namely,

$$M_n(s) = \frac{s}{s + \omega_t} M_V + k_n. \quad (5)$$

From now on, the distortion model will be given by (3) and (5). The model is characterized by two parameters: the bandwidth limitation due to the distant measurement, ω_t , and the sensor noise intensity, k_n . Note that perfect measurements correspond to $\omega_t = \infty$, and $k_n = 0$, and that the distortion increases with increasing k_n and decreasing ω_t . For illustration purposes, in this subsection, we set $\omega_t = 3.8$, $k_n = 3 \times 10^{-2}$ and investigate the influence of the resulting distortion on different aspects of preview control.

Remark 4: In practice, the parameters of the measurement distortion model should be identified using experimental data obtained from a real-world measurement setup. One way to perform identification is by using a Box Jenkins model [26] as discussed in Section V. Some more evolved models for M_t and M_n may also be considered, as well as non-parametric identification methods for the construction of M_t and M_n .

As a first step, consider the curve of the achievable performance as a function of the preview length presented in Figure 6. As expected, the performance improvement due to availability of preview has decreased compared to the case with pure measurements described in Figure 4. Another important observation is that the length of preview required to obtain 90% of the possible improvement has increased to 1 sec.

To further investigate the impact of measurement distortion on the preview control, we compare the behavior of the following three systems:

- 1) The system with a feedforward controller based on local measurements without preview. This controller will be denoted by K_0^d and is obtained by solving **OP** with $M_t = 1$ and $M_n = 3 \times 10^{-2}$, i.e., assuming that the measurements are corrupted with white additive noise only.
- 2) The system with a feedforward controller based on distant measurements with preview of $h = 1.3$ sec. This controller will be denoted by K_h^d and is obtained

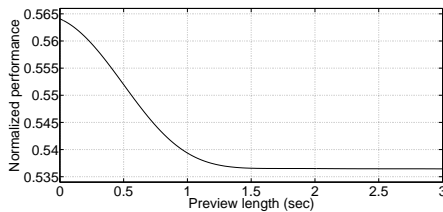


Fig. 6. Performance ($\|T\|_2$) vs. h (normalized with respect to the \mathcal{H}_2 -norm of the original system). Compared to the case with pure measurements (Figure 4), the improvement due to availability of preview has decreased and the required preview length has increased.

TABLE II
SIMULATION RESULTS BASED ON THE NONLINEAR TURBINE MODEL AND EWS ESTIMATED FROM REAL-WORLD DATA. (FEEDFORWARD BASED ON EWS MEASUREMENTS WITH DISTORTION.)

	DEL(M_t) kNm	DEL(M_b) kNm	max(β) deg/sec	max(P) kW	max(ω) rpm
K_0^d	1925	784	0.16	249	2.4×10^{-2}
K_h^d	1768	774	0.28	189	2.8×10^{-2}
K_h^p	2191	791	0.30	211	3.6×10^{-2}

by solving **OP** with M_t and M_n as in (3) and (5), respectively, with $\omega_t = 3.8$, $k_n = 3 \times 10^{-2}$.

- 3) The system with the a preview controller K_h^p from the previous subsection, which was obtained assuming perfect measurements. This controller is considered to demonstrate that ignoring distortions in the controller design may lead to a poor controller behavior.

Remark 5: The superscript d in K_0^d , K_h^d reflects that these controllers were synthesized accounting for the distortion in measurements.

We compare the response of these three systems to the effective wind speed estimated from real-world experimental data as explained in Section II-B. Note that in simulations we artificially distort the measurements with respect to the distortion model that corresponds to the preview length (i.e. to the distance between the turbine and the measurement location). Namely, in simulations with K_h^d and K_h^p the measurements are distorted with respect to (3), (5) with $\omega_t = 3.8$ and $k_n = 3 \times 10^{-2}$. In simulations with K_0^d , which uses the local measurements, the distortion is with respect to $M_t = 1$ and $M_n = 3 \times 10^{-2}$. As before, we run simulations on 10 different time series, each one minute long. The average outcome of these simulations is presented in Table II and the time series of one of the simulations are presented in Figure 7.

Comparing the behavior of K_0^d and K_h^d we see that, despite of the additional distortion associated with distant sensing, the use of preview is still beneficial. Note, however, that the decrease in the tower bending moment due to the use of preview is only 8.2%. This is substantially lower than

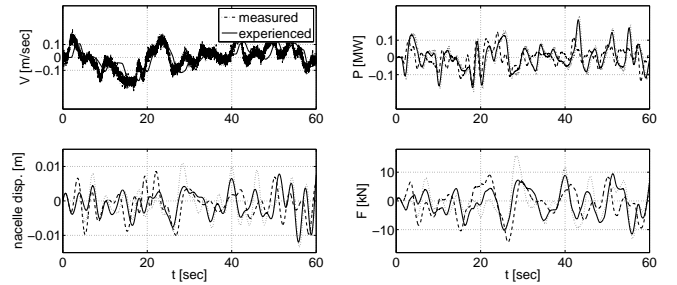


Fig. 7. Simulation results based on the nonlinear turbine model and EWS estimated from real-world data. The EWS measurements are artificially corrupted with respect to the distortion model. [solid — K_h^d ; dashed — K_0^d ; dotted — K_h^p] The average results of 10 simulations of this kind are summarized in Table II.

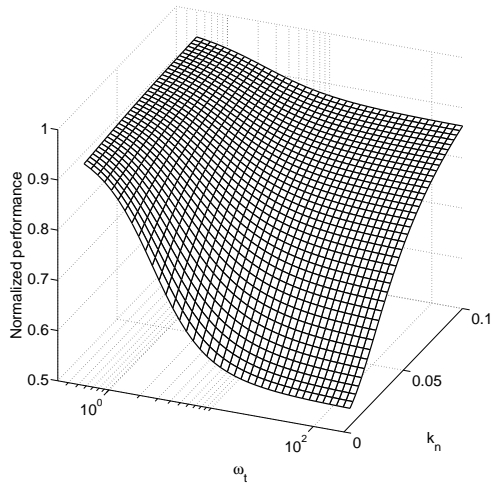


Fig. 8. Normalized performance that can be achieved with unlimited preview as a function of the distortion parameters. As expected, the performance monotonically improves with decreasing k_n and increasing ω_t .

the 31% that could be obtained in the previous subsection with perfect measurements.

Finally, the results obtained from the simulations with K_h^p deserve a separate discussion. These results demonstrate that accounting for measurement distortion at the stage of controller synthesis is crucial for obtaining an adequate system behavior. Indeed, we see that K_h^p , which was obtained ignoring the distortion, is outperformed not only by K_h^d but also by K_0^d . This suggests that in some situations not using preview might be better than using it without accounting for the distortion. Note, however, that the results still indicate that, in the considered example, having distorted previewed measurements might be advantageous if the distortion is taken into account.

C. Effects of measurement distortion on the achievable performance and the required preview length

Results from the previous subsection motivate further analysis of the relation between measurement distortion characteristics and different aspects of preview control. As a first step, we assume unlimited preview length, and plot the achievable performance as a function of the distortion model parameters, ω_t and k_n , see Figure 8. As expected, the performance monotonically improves with decreasing k_n and increasing ω_t . Also note that its normalized value approaches a value of approximately 0.4, which is consistent with Figure 4. The rapid deterioration in performance as ω_t decreases from 3 to 1 rad/sec can be related to the natural frequency of the tower, located at 2 rad/sec. Once ω_t decreases below this value, the frequencies responsible for tower excitation are filtered out of the measured signal V_m , which makes feedforward control based on these measurements irrelevant.

Another natural question is how the required preview length is affected by the distortion characteristics. Figure 9 shows the preview length required to attain 90% of all possible performance improvement as a function of ω_t and

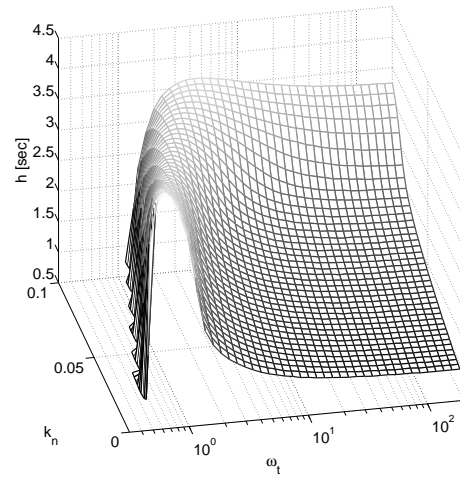


Fig. 9. The preview length required to attain 90% of all possible performance improvement as a function of the distortion parameters. We see that a longer preview is needed to cope with an increase in the measurement noise intensity. The same is true for a decrease in the bandwidth ω_t , but only up to a certain frequency after which there is a sharp decrease in the required preview length.

k_n . It shows that a longer preview is needed to cope with an increase in the sensor noise intensity. The same is true for a decrease in bandwidth ω_t , but only up to a certain frequency after which there is a sharp decrease in the required preview length. The decrease starts around 1 – 2 rad/sec, indicating that there is less to be done once frequencies related to the system dynamics are filtered out of the measurement.

V. PREVIEW FROM UPWIND TURBINES

So far, we have assumed that (possibly distorted) previewed effective wind speed measurements are available, but have said nothing about how to obtain them. One possibility would be to measure the wind field ahead of the turbine using LIDAR and estimate the effective wind speed from this data. In wind farms, there is yet another possibility: upwind turbines could be used as sensors for their downwind neighbors. If successful, this option would offer several benefits. First, it is cheap since it does not require additional hardware. Second, by definition the effective wind speed is best estimated via a turbine.

To assess the potential of using upwind turbine measurements for preview control, we identify the corresponding measurement distortion model M_n and M_t based on real wind turbine data collected from OWEZ wind farm. The data was collected from two neighboring turbines. During the data collection the mean wind speed was 10 m/s and the mean wind direction was from one turbine to the other. For more information on the data set, see [16] where it is described in detail.

Effective wind speeds at both turbines were estimated from the data as described in [16] and used as inputs to the identification procedure. To be consistent with earlier notations, the effective wind speeds at the upwind and downwind turbines are denoted V_m and V_i , respectively. See Figure 3.

The relation between the signals is $V_m = M_t V + M_n n = M_t e^{sh} V_i + M_n n$, where h is the delay and n is a white noise process, independent of V . The delay was estimated using covariance estimates and prewhitening [18]. This resulted in a delay estimate of 60 sec, which is slightly smaller than the time it would take to travel between the turbines at mean wind speed. After setting $h = 60$ s, a prediction error method was used to fit M_t and M_n to a Box Jenkins model structure, [26]. This resulted in a bandwidth for M_t of $\omega_t = 0.015$, which is far below the 2 rad/sec needed to obtain a significant performance improvement. This shows that, effective wind speed estimates from a single upwind turbine are not useful for reducing tower oscillations, at least not for the wind conditions during the data collection. Indeed, substituting the identified M_t and M_n into the solution of **OP** yielded only an improvement of 0.8% in terms of the performance index.

Although the outcome of this section is negative, it provides us with insights for future research. The results suggest that in order to benefit from preview, effective wind speeds must be based on measurements close to the turbine. Note that, measuring closer to the turbine is feasible in terms of preview length, since the amount of preview needed is only a number of seconds.

VI. CONCLUDING REMARKS

In this paper, we considered the possibility of using previewed wind speed measurements for damping tower oscillations. Recent results on continuous-time H^2 preview control were used in order to develop a convenient framework for the analysis of the problem and for controller synthesis. The resulting controller performance was demonstrated by means of simulations based on the nonlinear NREL 5 MW turbine model described in [13], [14] and wind speeds obtained from real-world measurements.

We showed that in case of perfect measurements, a 31% improvement in terms of the damage equivalent load can be achieved due to availability of 1.3 sec preview. However, the benefit of using preview decreases in presence of measurement distortion. As expected, we saw that previewed measurements are useful only if their bandwidth exceeds the natural frequency of the tower. We also realized that, although the required length of preview grows due to the presence of measurement distortions, it does not exceed 5 sec for a reasonable range of distortion parameter values.

It is worth emphasizing that in the proposed control methodology, the model of the measurement distortion is naturally incorporated in the problem formulation. In other words, the distortion is explicitly taken into account during the controller synthesis. As demonstrated in Section IV, this is important for obtaining adequate controller behavior. In particular, we showed that in some cases it might be better not to use previewed information rather than using it without appropriately accounting for the distortion.

REFERENCES

- [1] L. Y. Pao and K. E. Johnson, "A tutorial on the dynamics and control of wind turbines and wind farms," in *Proceedings of American Control Conference*, June 2009, pp. 2076–2089.
- [2] J. H. Laks, L. Y. Pao, and A. D. Wright, "Control of wind turbines: Past, present, and future," in *Proceedings of American Control Conference*, July 2009, pp. 2096–2103.
- [3] D. Schlipf, S. Schuler, F. Allgower, and M. Kuhn, "Look-ahead cyclic pitch control with lidar," in *Proc. The Science of Making Torque from Wind*, Heraklion, Greece, June 2010.
- [4] A. Korber and R. King, "Model predictive control for wind turbines," in *European Wind Energy Conference*, April 2010.
- [5] M. Soltani, R. Wisniewski, P. Brath, and S. Boyd, "Load reduction of wind turbines using receding horizon control," in *Proc. IEEE International Conference on Control Applications*, Denver, CO, USA, Sep. 2011.
- [6] J. Laks, L. Y. Pao, E. Simley, A. D. Wright, N. Kelley, and B. Jonkman, "Model predictive control using preview measurements from lidar," in *AIAA Aerospace Sciences Meeting*, Orlando, FL, Jan 2011.
- [7] J. Laks, L. Pao, A. Wright, N. Kelley, and B. Jonkman, "The use of preview wind measurements for blade pitch control," *Mechatronics*, vol. 21, no. 4, pp. 668–681, June 2011.
- [8] F. Dunne, L. Y. Pao, A. D. Wright, B. Jonkman, and N. Kelley, "Adding feedforward blade pitch control to standard feedback controllers for load mitigation in wind turbines," *Mechatronics*, vol. 21, no. 4, pp. 682–690, June 2011.
- [9] N. Wang, K. E. Johnson, and A. D. Wright, "FX-RLS-based feedforward control for LIDAR-enabled wind turbine load mitigation," to appear in *IEEE Transactions On Control Systems Technology*, 2012.
- [10] M. Kristalny and L. Mirkin, "On the H^2 two-sided model matching problem with preview," to appear in *IEEE Transactions On Automatic Control*, 2011.
- [11] M. Kristalny and D. Madjidian, "Decentralized feedforward control of wind farms: prospects and open problems," in *Proc. 50th IEEE Conference on Decision and Control*, Orlando, FL, Dec. 2011.
- [12] L. Mirkin, "On the fixed-lag smoothing: How to exploit the information preview," *Automatica*, vol. 39, no. 8, pp. 1495–1504, 2003.
- [13] J. Jonkman, S. Butterfield, W. Musial, and G. Scott, "Definition of a 5-MW reference wind turbine for offshore system development," National Renewable Energy Laboratory, Golden, Colorado, Tech. Rep., Feb 2010.
- [14] J. D. Grunnet, M. Soltani, T. Knudsen, M. Kragelund, and T. Bak, "Aeolus toolbox for dynamic wind farm model, simulation and control," in *Proc. of the 2010 European Wind Energy Conference*, 2010.
- [15] V. Spudic, M. Jelavic, M. Baotic, and N. Peric, "Hierarchical wind farm control for power/load optimization," in *Proc. of Torque*, Heraklion, Greece, June 2010.
- [16] T. Knudsen, M. Soltani, and T. Bak, "Prediction models for wind speed at turbine locations in a wind farm," *Wind Energy*, vol. 14, pp. 877–894, 2011, published online in Wiley Online Library (wileyonlinelibrary.com). DOI: 10.1002/we.491.
- [17] "Egmond aan zee offshore wind farm," Internet <http://www.noordzeewind.nl/>, 12 2009, <http://www.noordzeewind.nl/>.
- [18] L. Ljung, *System Identification, Theory for the User*, 2nd ed., ser. Prentice-Hall information and system sciences series. Prentice-Hall, 1999.
- [19] T. Burton, D. Sharpe, N. Jenkins, and E. Bossayani, *Wind Energy Handbook*. John Wiley & Sons, 2008.
- [20] J. Jonkman, "NWTC Design Codes (FAST)." [Online]. Available: <http://wind.nrel.gov/designcodes/simulators/fast/>
- [21] "SimWindFarm." [Online]. Available: <http://www.ict-aeolus.eu/SimWindFarm/>
- [22] K. Hammerum, P. Brath, and N. K. Poulsen, "A fatigue approach to wind turbine control," *Journal of Physics: Conference Series*, vol. 75, 2007.
- [23] M. O. L. Hansen, *Aerodynamics of Wind Turbines*, 2nd ed. Earthscan, 2008.
- [24] H. A. Panofsky and J. A. Dutton, *Atmospheric Turbulence*. John Wiley & Sons, 1984.
- [25] E. Simley, L. Y. Pao, N. Kelley, B. Jonkman, and R. Frehlich, "Lidar wind speed measurements of evolving wind fields," in *Proc. AIAA Aerospace Sciences Meeting*, in press, Nashville, TN, Jan 2012.
- [26] G. E. P. Box and G. M. Jenkins, *Time Series Analysis, Forecasting and Control*. San Francisco: Holden Day, 1976.